

Quantitative PCR for Determining the Infectivity of Bacteriophage MS2 upon Inactivation by Heat, UV-B Radiation, and Singlet Oxygen: Advantages and Limitations of an Enzymatic Treatment To Reduce False-Positive Results[∇]

Brian M. Pecson,* Luisa Valério Martin, and Tamar Kohn

Environmental Science and Technology Institute, Ecole Polytechnique Fédérale de Lausanne, 1015 Lausanne, Switzerland

Received 20 February 2009/Accepted 2 July 2009

Health risks posed by waterborne viruses are difficult to assess because it is tedious or impossible to determine the infectivity of many viruses. Recent studies hypothesized that quantitative PCR (qPCR) could selectively quantify infective viruses if preceded by an enzymatic treatment (ET) to reduce confounding false-positive signals. The goal of this study was to determine if ET with qPCR (ET-qPCR) can be used to accurately quantify the infectivity of the human viral surrogate bacteriophage MS2 upon partial inactivation by three treatments (heating at 72°C, singlet oxygen, and UV radiation). Viruses were inactivated in buffered solutions and a lake water sample and assayed with culturing, qPCR, and ET-qPCR. To ensure that inactivating genome damage was fully captured, primer sets that covered the entire coding region were used. The susceptibility of different genome regions and the maximum genomic damage after each inactivating treatment were compared. We found that (i) qPCR alone caused false-positive results for all treatments, (ii) ET-qPCR significantly reduced (up to >5.2 log units) but did not eliminate the false-positive signals, and (iii) the elimination of false-positive signals differed between inactivating treatments. By assaying the whole coding region, we demonstrated that genome damage only partially accounts for virus inactivation. The possibility of achieving complete accord between culture- and PCR-based assays is therefore called into doubt. Despite these differences, we postulate that ET-qPCR can track infectivity, given that decreases in infectivity were always accompanied by dose-dependent decreases in ET-qPCR signal. By decreasing false-positive signals, ET-qPCR improved the detection of infectivity loss relative to qPCR.

Water- and food-borne viruses are a major worldwide source of gastroenteritis, and thus the detection and inactivation of infective viruses are important public health priorities. Cell culture can be employed to quantify the infectivity of certain viruses. However, culturing can take days to weeks to yield results, and many viruses important to public health, e.g., hepatitis A and noroviruses, are either difficult to culture or are nonculturable (3, 19, 38). Immunological and spectrometry- and microscopy-based methods have also been developed, but none of them has provided a satisfactory alternative (5, 26, 43, 45).

The advent of PCR and quantitative PCR (qPCR) in environmental microbiology had raised hopes that these limitations would be overcome. While PCR lives up to its promise to provide rapid, sensitive, and specific detection of environmental viruses, its ability to differentiate infective from inactivated viruses has not been realized. This is mainly due to the persistence of genomes of inactivated viruses that remain either partially or fully intact. During PCR, intact genomic regions of inactivated viruses are amplified and produce confounding false-positive PCR signals (3, 11, 37, 38, 41). These false positives inhibit our ability to use qPCR to obtain quantitative information on infectivity, which constitutes the major limita-

tion of the method. Adapting qPCR protocols to provide quantitative information is the crucial next step in its advancement. Only with quantitative information can one measure the pathogenic potential of an environmental sample or determine whether a virus-inactivating treatment has met regulatory limits.

Various strategies have been used to improve the capabilities of PCR, but no method to date has produced a quantitative measure of infectivity. These strategies include using multiple PCR sites (41), longer amplicons (11, 39, 41), and immunocapture PCR (41). One method that has shown promise in selectively detecting infective RNA viruses is integrated cell culture/strand-specific reverse transcription-PCR (7, 18) though, again, this method includes a culture-based step that is not available for many viruses.

Nuanualsuwan and Cliver (27) showed that false-positive PCR signals were eliminated after subjecting inactivated viruses to an enzymatic treatment (ET) with proteinase K and RNase prior to nucleic acid extraction and PCR. In theory, the ET differentiates infective from inactivated viruses based on differences in the ability of their protein capsids to protect the genomes from proteases and RNase. Increased proteolytic susceptibility has been shown for proteins damaged by both heat (8) and reactive oxygen species (ROS) (31); therefore, the ET should more readily degrade the capsids of viruses inactivated by either of these methods. With the capsid degraded, the naked RNA is more susceptible to RNase degradation than capsid-enclosed RNA (28).

* Corresponding author. Mailing address: Environmental Science and Technology Institute, Ecole Polytechnique Fédérale de Lausanne, 1015 Lausanne, Switzerland. Phone: 41 21 693 8025. Fax: 41 21 693 6390. E-mail: bmpecson@gmail.com.

[∇] Published ahead of print on 10 July 2009.

Nuanualsuwan and Cliver used standard PCR, not qPCR, and thus had semiquantitative results (post-PCR comparison of PCR band intensities on electrophoresis gels) (27, 28). Various authors have suggested that coupling the ET with genome-based methods might yield quantitative results (11, 27); however, studies that have tested ET-qPCR have reported both positive (21) and negative results (1, 30). qPCR without ET is also increasingly used to quantify virus infectivity (2, 3) though, again, the studies come to contradictory conclusions regarding its usefulness. A recent review article has emphasized the need for quantitative measures of viral infectivity and has highlighted ET-qPCR as one of the techniques with the most potential (33). We have therefore attempted to do a systematic evaluation of qPCR as a tool to quantify MS2 infectivity.

Many fundamental questions regarding the use of qPCR to determine infectivity remain unanswered. Most importantly, few studies have compared how much of the inactivation results from damage to the genome, compared to damage to the capsid and the host attachment site. This question is of utmost priority because PCR is a method that measures genomic integrity and thus may be limited by its inability to measure inactivation due to nongenomic damage. Furthermore, it is not known if certain genome sections are preferentially damaged compared to others that might be protected from the inactivating agent. And lastly, how efficiently does ET degrade the capsids damaged by different treatments and thereby allow degradation of the (possibly intact) genome by RNase?

The goal of this research was to assess the use of qPCR and ET-qPCR to quantify the infectivity of bacteriophage MS2. In particular, we focused on (i) determining the susceptibility of different genome regions to inactivation by heat, singlet oxygen, and UV radiation; (ii) quantitatively relating the loss of qPCR signal to the loss of infectivity after inactivation; and (iii) determining if ET improved the correspondence between qPCR and culturing, in particular, upon only partial inactivation.

MS2 is an RNA bacteriophage that is frequently used as a surrogate for human viruses and can be easily cultured to determine infectivity (10, 15, 22, 25, 38). This latter characteristic aided the optimization process by providing an infectivity standard against which to compare the qPCR and ET-qPCR methods. The treatments were chosen for their different mechanisms of inactivation (i.e., physical deformation, oxidative damage, and production of photoproducts) and their relevance to public health and environmental fate (i.e., virus inactivation during pasteurization and UV disinfection and photo-inactivation within sunlight-exposed surface waters) (4).

MATERIALS AND METHODS

Experimental approach. In brief, the experimental section was divided into three distinct phases. In the first phase, qPCR was used to assay damage to the entire coding region following highly inactivating treatments. This phase allowed us to identify the genomic regions that were most susceptible to the different forms of inactivation. Second, we conducted time courses with three inactivating treatments to obtain different levels of virus inactivation. Following inactivation over time allowed us to compare the responses of different detection methods (culturing, standard qPCR, and ET-qPCR) to various levels of inactivation, from completely infective samples to those with $>8 \log_{10}$ inactivation. In the third phase we tested our findings in a lake water matrix to ensure the applicability of our findings to an environmental sample.

TABLE 1. Primer sets used for qPCR amplification of the MS2 genome^a

Primer set	Direction	Primer sequence (5'-3')	MS2 target location (nucleotide position)
1	Forward	TGTCTTTAGCGAGACGCTACC	59–371
	Reverse	GATGACCCACTTCGCTTGTAG	
2	Forward	AAGGTGCCTACAAGCGAAGT	344–678
	Reverse	TTCGTTTAGGGCAAGGTAGC	
3	Forward	CCGCTACCTTGCCCTAAAC	657–959
	Reverse	GACGACAACCATTGCCAAAC	
4	Forward	GCATGGTTGTCGTCTCTAGGT	946–1246
	Reverse	ACTTTACGTACGCAGCCAGTT	
5	Forward	AACTGGCGCGTACGTAAAGT	1227–1529
	Reverse	CACCTCGACTTTGATGGTGTA	
6	Forward	CCTAAAGTGGCAACCCAGAC	1530–1818
	Reverse	AAAGATCGCGAGGAAGATCA	
7	Forward	CGCGATCTTTCTCTCGAAAT	1809–2125
	Reverse	GACGATCGGTAGCCAGAGAG	
8	Forward	CTACCGATCGTCTGTTGTTTG	2114–2420
	Reverse	GACCCCTTTCTGGAGGTACA	
9	Forward	GGTCGGTGCTTTTCATCAGA	2417–2723
	Reverse	TGCCCAGAATATCATGGACTC	
10	Forward	ATAGTCAAAGCGACCCAAATC	2724–3033
	Reverse	GGCGTGGATCTGACATACCT	
11	Forward	ATGTCAGATCCACGCCTCTA	3018–3304
	Reverse	TTCATGCTGTCGGTGATTC	
12	Forward	GAAATCACCGACAGCATGAA	3285–3528
	Reverse	AATCCCGGGTCTCTCTTTA	

^a The total genome size is 3,569 nucleotides (NCBI accession number NC_001417).

Microorganisms. Bacteriophage MS2 and its *Escherichia coli* host were purchased from the German Collection of Microorganisms and Cell Cultures (DSMZ numbers 13767 and 5695, respectively; Braunschweig, Germany). Virus was propagated in *E. coli* and subsequently purified and concentrated in different steps. The virus was initially inoculated into 1 liter of LB medium (10 g of Bactotryptone; Becton Dickinson, Sparks, MD), 1 g of yeast extract (Fisher, Wohlen, Switzerland), 8 g of NaCl (99.5%; Acros Organics) supplemented with 1 g of D-glucose (Acros Organics), 0.3 g of CaCl₂ (+99%; Acros Organics), and 2 mg of streptomycin sulfate (Sigma Aldrich, St. Louis, MO) containing log-phase *E. coli* at roughly 10⁷ CFU/ml at a multiplicity of infection of 0.1. Five hours postinoculation, the liter of bacterial-viral suspension was mixed with 5 ml of chloroform to complete the lysis of all bacteria. The suspension was centrifuged for 15 min at 4,000 × g to separate the bacterial debris from the virus, and the resulting supernatant was stored overnight at 4°C with 10% polyethylene glycol (PEG 6000; Sigma Aldrich) and 0.5 M NaCl. The PEG solution was centrifuged at 7,000 × g for 45 min, and the virus-containing pellet was resuspended into 35 ml of dilution buffer (DB) (5 mM NaH₂PO₄ [+99% Acros Organics], 10 mM NaCl, pH 7.4). The PEG was removed by centrifugation at 10,000 × g and extracted with chloroform. The remaining aqueous phase was centrifuged for 10 min at 3,000 × g to separate it from the organic phase, transferred to a new tube, and sparged with air to volatilize any remaining chloroform. Finally, the sample was concentrated in an Amicon Ultra centrifugal filter device (100,000 Da nominal molecular weight limit), washed three times with DB in the same filter, and then passed through a 0.1-μm-pore-size polyvinylidene difluoride filter (Millipore, Billerica, MA). Infective MS2 was quantified using a double-layer agar technique as described previously (4, 20), and infective virus concentrations were measured as the number of PFU per ml.

RNA extraction. RNA was extracted from 200-μl samples of MS2 using a PureLink Viral RNA/DNA extraction kit (Invitrogen, Carlsbad, CA) according to the manufacturer's instructions. Extracted RNA was eluted using 50 μl of RNase-/DNase-free water (supplied with the kit).

Primers. All the primers used in this project were designed with the Primer3 free, online software (<http://primer3.sourceforge.net/>) and synthesized by Microsynth (Balgach, Switzerland). Twelve sets of primers targeting roughly 300 nucleotide segments were developed to cover the entire coding region of MS2 (Table 1). The complete genome of MS2 was taken from the NCBI GenBank database (www.ncbi.nlm.nih.gov; accession number NC_001417).

Development of MS2 whole-genome RNA standards. Whole-genome standards for qPCR were created by extracting RNA from a concentrated stock of MS2. The mass of the extracted RNA was determined fluorometrically (Qubit fluorometer with Quant-iT RNA Assay Kit; Invitrogen), and the integrity of the extracted RNA was verified electrophoretically (2100 Bioanalyzer, Agilent, Palo Alto, CA). The copy number per volume was calculated assuming a genome of 3,569 nucleotides and an average molecular mass of 330 Da per nucleotide. The initial stock solution was serially diluted to give standard concentrations from 10^1 to 10^7 copies per 15- μ l reaction volume.

qPCR. Experimental samples and RNA standards were reverse transcribed and amplified in parallel using a RotorGene 3000 qPCR platform (Corbett Life Science, Sydney, Australia). Each reverse transcription-qPCR sample was run in 15 μ l of total volume comprising 7.5 μ l of 2 \times SensiMix One-Step, 0.3 μ l of 50 \times SYBR Green I solution, 0.3 μ l of RNase inhibitor solution, 0.3 μ l each of 10 μ M forward and reverse primers, 3.3 μ l of water, and 3 μ l of RNA sample (Quantace Ltd., London, United Kingdom). The following thermocycling conditions were used: 30 min at 49°C; 10 min at 95°C; and 45 cycles of 95°C for 15 s, 60°C for 35 s, and 72°C for 40 s, followed by a melting ramp from 72 to 95°C, with holding for 45 s on the first step (72°C) and 5-s holds on all subsequent temperatures. The genome copies/ml in the original sample were calculated by dividing the qPCR results (in total genome copies) by the volume of the extracted sample used in each qPCR reaction mixture (total genome copies per 3 μ l of extraction) and accounting for the fourfold concentration during the RNA extraction (from an initial 200- μ l sample to 50 μ l). The detection limit for a given primer set was determined according to a modified version of the method of Hubaux and Vos, with a 95% confidence level (17). In brief, the detection limits were determined by relating the qPCR output, the cycle threshold (C_T) number, to the known amount of standard. Because the C_T values were inversely related to standard levels (i.e., lower quantities of standards corresponded to higher C_T values), the only modification for determining the detection limit consisted in subtracting all C_T values from a maximum C_T value of 40, the maximum number of amplification cycles used for the qPCR.

ET. For the ET, MS2 samples containing 10^{10} PFU/ml were mixed with both proteinase K (333 U/ml; Promega, Madison, WI) and a purified stock of RNase A (230 mU/ml; Invitrogen, Carlsbad, CA). The treatment consisted of incubating the samples with the enzymes for 30 min at $37.0 \pm 0.2^\circ\text{C}$ in a water bath (model TW12; Julabo, Seelbach, Germany). Control experiments verified that the ET did not cause a significant reduction in MS2 infectivity measured by culturing.

Inactivating treatments. All inactivating treatments were performed in triplicate, with an initial MS2 concentration of 10^{10} PFU/ml in DB. After inactivation, samples were divided into three parts for culturing, RNA extraction, and ET followed by RNA extraction. Sample manipulation was performed immediately following the inactivating treatment.

Heat treatment. MS2 samples were heated to 72°C in thin-walled, 500- μ l tubes in a PCR thermocycler (PTC-200 DNA Engine; MJ Research, South San Francisco, CA) for the specified lengths of time and then immediately removed to an ice bath.

UV inactivation. MS2 samples were pipetted into 1.5-ml microcentrifuge tubes and placed 5 cm below a 30-W, germicidal UV lamp (model G30T8; 2.7 ± 0.3 mW/cm² irradiance at 253.7 nm wavelength; Sankyo Denki, Tokyo, Japan) for 1 to 4 min. The UV irradiance was measured by actinometry, as described elsewhere (32). UV radiation exposures of 1 to 4 min were equivalent to 1,900, 3,200, 4,400, and 5,900 J/m², respectively. The lowest dose tested is roughly identical to the minimum UV dose required by the U.S. Environmental Protection Agency (1,860 J/m²) for virus disinfection of drinking water (44).

Singlet oxygen inactivation. MS2 samples were pipetted into glass beakers with magnetic stirring rods and placed in a plastic, water-filled tray atop a multipoint magnetic stir plate (Poly 15; Thermo Scientific Variomag, Waltham, MA) that was cooled with a recirculating cooler to maintain the temperature in the beakers at 20°C (F240 Recirculating Cooler; Julabo, Seelbach, Germany). The entire cooling/stirring system was placed under a Sun 2000 Solar Simulator (ABET Technologies, Milford, CT) equipped with a 1,000-W Xe lamp, an AM1.5 and a UV-B/C cutoff filter. The total irradiance up to 800 nm for this setup was determined spectroradiometrically (model ILT-900-R; International Light) and was 300 W/m². Rose Bengal (85% purity; Acros Organics) was added to a final concentration of 0.5 mg/liter every 30 min during the exposure period. This procedure resulted in a constant singlet oxygen concentration of 4×10^{-12} M, as determined by reaction of singlet oxygen with a selective probe compound (20). Control experiments verified that the presence of rose bengal and its photoproducts after 4 h of exposure to the solar simulator had no inhibitory effect on the downstream reverse transcription or qPCR.

Comparison of assays with environmental water samples. UV inactivation experiments were also conducted with purified MS2 spiked into both dilution

buffer and 0.45- μ m-pore-size-filtered water samples taken from Lake Geneva, Switzerland. Fifty-milliliter samples were spiked with 10^8 PFU/ml of MS2 before exposure to UV radiation. Samples were taken during a 2-min UV exposure, and viruses were concentrated 100 times using a 100-kDa Amicon Ultra centrifugal filter. Following the concentration step, samples were cultured and assayed with both qPCR and ET-qPCR.

Data interpretation. Triplicate samples were run with both the culturing and qPCR assays. Sample replicates were log transformed and averaged, and the 95% confidence interval was determined. The normalized loss of infectivity or qPCR signal was determined with the following equation: $\log \text{inactivation} = \log C_{0,\text{avg}} - \log C_{x,\text{avg}}$, where $\log C_{0,\text{avg}}$ and $\log C_{x,\text{avg}}$ are the average log concentrations of virus or genomic targets in the time zero control and in the experimental samples at time x . First-order inactivation rate constants were determined by linear regression of the natural-log-transformed inactivation data versus time. All rate constants are expressed as mean \pm 95% confidence interval.

RESULTS

Assessment of damage to MS2 coding region. Inactivated MS2 samples (10^{10} PFU/ml initial concentration) were used to identify which genomic regions were most susceptible to the different treatments and to compare the loss in genomic amplification with the loss in infectivity measured with culturing. The loss of qPCR signal across the entire coding region was quantified for samples with and without ET using 12 primer sets (Fig. 1). A comparison of the signal loss revealed a number of points. First, in the absence of ET, no single primer set alone caused a loss of signal that was equivalent to the loss of infectivity measured with culturing (Table 2). The addition of the ET to the protocol decreased the signal in 31 of 35 samples tested (primer set 11 from the singlet oxygen data could not be analyzed due to the detection limits). However, the ET-induced loss of qPCR signal was dependent on the inactivating treatment that preceded it. For both the heat and UV inactivation, the ET caused significant losses in the qPCR signal for all 12 primer sets tested (Fig. 1a and c). For singlet oxygen inactivation, however, only 7 of the 11 comparable samples showed significant loss of signal (primer set 11 excluded) (Fig. 1b). Although the ET decreased the signals, the ET-qPCR still significantly underestimated the loss in infectivity measured with culturing.

The qPCR data were also used to calculate the total signal loss across the entire coding region. To make this calculation, we made the conservative assumption that no virus was damaged in more than one primer-delimited region at one time. Under these circumstances, the total inactivation is simply the summation of the signal loss in each of the 12 regions (Table 2).

Comparison of culturing with qPCR and ET-qPCR: time course results. With the initial qPCR data, we selected the primer sets that showed the best combination of (i) high levels of qPCR signal loss after the ET, (ii) sensitivity (i.e., the lowest limit of detection), and (iii) specificity (i.e., the absence of extraneous amplicons and primer-dimers in the melt curves of the qPCR products). Note that during primer design, the most important criterion was that the coding region be completely covered with minimal overlap between adjacent segments. Because of this design restriction, the primer sets were not equally optimized for sensitivity.

The optimum primers corresponded to set 3 for the UV-treated samples and to set 12 for the singlet oxygen and heat-treated samples. Time courses were run for each of the three

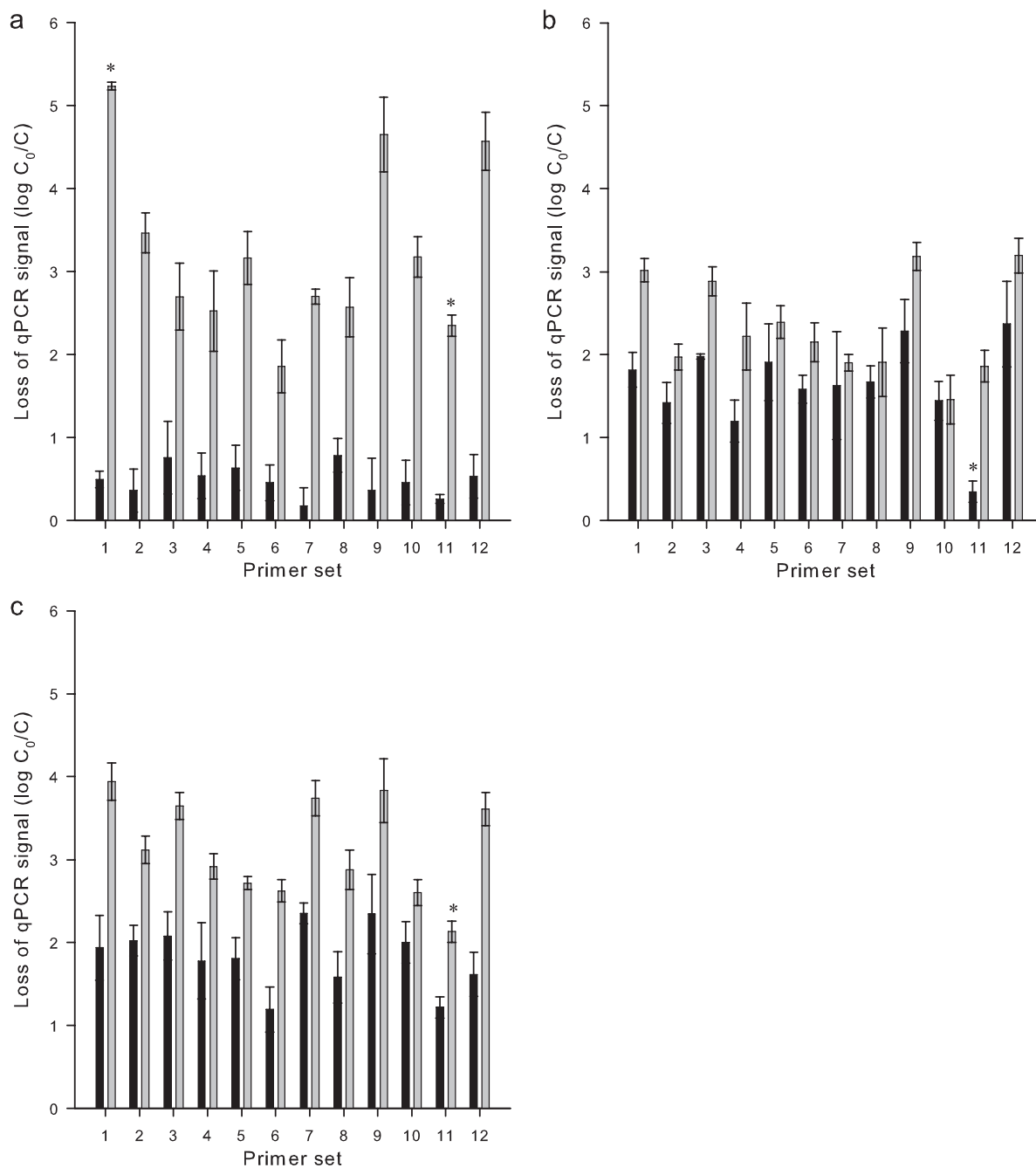


FIG. 1. Loss of qPCR signals in different regions of the MS2 genome both without (black bars) and with (gray bars) ET following inactivation by heating at 72°C for 3 min (a), singlet oxygen for 4 h (b), and UV irradiation for 4 min (c). Error bars depict 95% confidence intervals; asterisks signify values below the detection limit. Table 1 gives the locations of the various primer sets.

inactivating treatments, and infectivity was assayed with culturing, qPCR alone, and ET-qPCR. The results of these experiments are presented in Fig. 2. Each of the treatments caused a significant and time-dependent decrease in infectivity measured by culturing and ET-qPCR. The qPCR also showed time-dependent losses in signal, except for the heat-treated sample (Fig. 2a). The first-order inactivation rate constants were determined for each treatment and infectivity assay (Fig. 3).

Signal loss in the heat-treated ET-qPCR samples leveled off after reaching roughly 4.5 log units. This phenomenon was verified with two other heat inactivation experiments (data not shown). Accordingly, only the data points from 0 to 2 min were used to determine the rate constant for this sample. In addition, only the positive culturing results were used in the linear regression (i.e., those results with at least one detectable PFU), which excluded the culturing results for the singlet oxygen at 180 min and the UV sample at 4 min. In the absence of a

TABLE 2. Effect of inactivating treatments on the infectivity and qPCR amplification of the MS2 genome

Inactivating treatment	Length of treatment	Loss of infectivity (log C_0/C)	qPCR signal loss per primer set (log C_0/C)		Sum of qPCR loss with 12 primer sets [log ($\Sigma C_0/C$)]	
			Without ET	With ET	Without ET	With ET
72°C	3 min	8.6 ± 0.4	0.18–0.78	1.9–5.2 ^a	1.6 ± 0.1	5.4 ± 0.1
Singlet oxygen	4 h	>10.8	1.2–2.4	1.5–3.2	2.9 ± 0.2	3.8 ± 0.1
UV radiation	4 min	8.7 ± 0.1	1.2–2.4	2.6–3.9	3.0 ± 0.1	4.5 ± 0.1

^a Value beyond the limit of detection.

detectable PFU, the detection limit was calculated as 1 PFU on the lowest dilution tested.

For the heat-inactivated samples, the first-order rate constants for culturing ($6.8 \pm 2.4 \text{ min}^{-1}$) and ET-qPCR ($5.2 \pm 1.3 \text{ min}^{-1}$) were not statistically different from each other but were both significantly higher than the qPCR constant ($0.10 \pm 0.39 \text{ min}^{-1}$) (Fig. 2a and 3a), which was not statistically different from zero. For inactivation by singlet oxygen, culturing results showed a significantly higher inactivation rate constant ($0.15 \pm 0.059 \text{ min}^{-1}$) than the ET-qPCR ($0.037 \pm 0.023 \text{ min}^{-1}$) and qPCR results ($0.034 \pm 0.024 \text{ min}^{-1}$) (Fig. 2b and 3b), which were not statistically different from each other. The level of UV inactivation measured with culturing was significantly higher than the qPCR signal loss for each time point tested (Fig. 2c). However, the first-order inactivation model did not fit the culturing data well; therefore, the rate constant is associated with high confidence intervals ($6.5 \pm 5.1 \text{ min}^{-1}$). Thus, the rate constants for ET-qPCR ($2.5 \pm 0.044 \text{ min}^{-1}$) and qPCR ($1.3 \pm 0.47 \text{ min}^{-1}$) were not statistically different from the culturing constant although their mean values were two to three times lower than the culturing values (Fig. 3c). Between the two qPCR samples, the ET-qPCR samples had higher inactivation for all time points after 1 min (Fig. 2c), and the corresponding rate constant was significantly higher than the sample measured with qPCR alone (Fig. 3c).

Comparison of infectivity assays with the environmental water sample. The ET-qPCR was also tested with a water sample from Lake Geneva, Switzerland, to determine if an environmental matrix would alter the relationship between culturing and qPCR and ET-qPCR compared to a “clean” buffer solution. Fifty-milliliter samples of both buffered solution and Lake Geneva water (LGW) were spiked with 10^8 PFU/ml, and the samples were exposed to UV irradiation, concentrated 100-fold, and tested by culturing, qPCR, and ET-qPCR. The loss of infectivity and of qPCR and ET-qPCR signals is shown in Fig. 4a, and the corresponding inactivation rate constants are shown in Fig. 4b. For all of the assays tested, the inactivation rate constants obtained in the LGW samples were not statistically different from those obtained in the dilution buffer.

DISCUSSION

Susceptibility of different genome regions to degradation.

The 12 primer sets were used to measure the susceptibility of the genome to degradation. In comparing the different regions, we found that there was a high level of variability both across the entire genome for a given treatment and across treatments for a specific genome region (Fig. 1). We hypothesize that this

variability arises primarily from differences in the structure of the genome that render some sections more susceptible than others. Both the degree of secondary structure and the level of genomic association with proteins are known to influence genomic susceptibility to degradation. The genome of MS2 has a complex secondary structure (12, 13) and is connected to the capsid at both the 5' and 3' ends via the A protein (36). Both of these factors have been shown to confer a higher resistance to ribonucleases and may explain why certain regions are more or less susceptible than others. Differences were also seen across inactivating treatments. For example, the heat-treated MS2 showed the highest level of genomic degradation with the ET. We hypothesize that the heat caused both denaturation of the protein capsid and decreased genomic secondary structure, allowing more effective degradation by the protease and RNase. The net result would therefore be a higher level of degradation than a treatment that did not cause equivalent levels of denaturation, e.g., UV radiation. A further analysis into the structure or stability of the different genomic regions and their susceptibility to different inactivating treatments may provide interesting insights.

Relationship between loss of infectivity and loss of qPCR and ET-qPCR signal. A limitation of previous ET-qPCR studies is the use of inactivating treatments that cause complete inactivation of the viruses, i.e., inactivation beyond the limits of detection (21, 27, 30). Treatments that cause complete inactivation of viral populations may cause greater destruction of the viruses than treatments that cause intermediate levels of inactivation. For example, heating of hepatitis A, poliovirus, and feline calicivirus to 72°C followed by ET resulted in complete elimination of the PCR signal, whereas a gentler treatment at 37°C did not (28). Thus, the ability of the method to selectively detect infective viruses in the presence of inactivated viruses was unclear. In this work, we overcame this shortcoming by utilizing time course experiments that gave us a range of inactivation levels from fully infective to >10 logs of inactivation.

At least three conditions are necessary for viral infectivity. (i) The genomic integrity must be sufficient to produce the proteins necessary for replication and to provide an accurate genetic template for subsequent generations. In addition, the capsid must be sufficiently intact to (ii) protect the genome from degradation and (iii) recognize and infect the appropriate host cell (28). Disrupting any of these three functions will adversely affect infectivity. The ET-qPCR assays the first two functions by measuring the integrity of the genome and the ability of the capsid to protect it from enzymatic degradation. In fact, the onset of susceptibility to exogenous RNases has previously been used to indicate capsid damage (24).

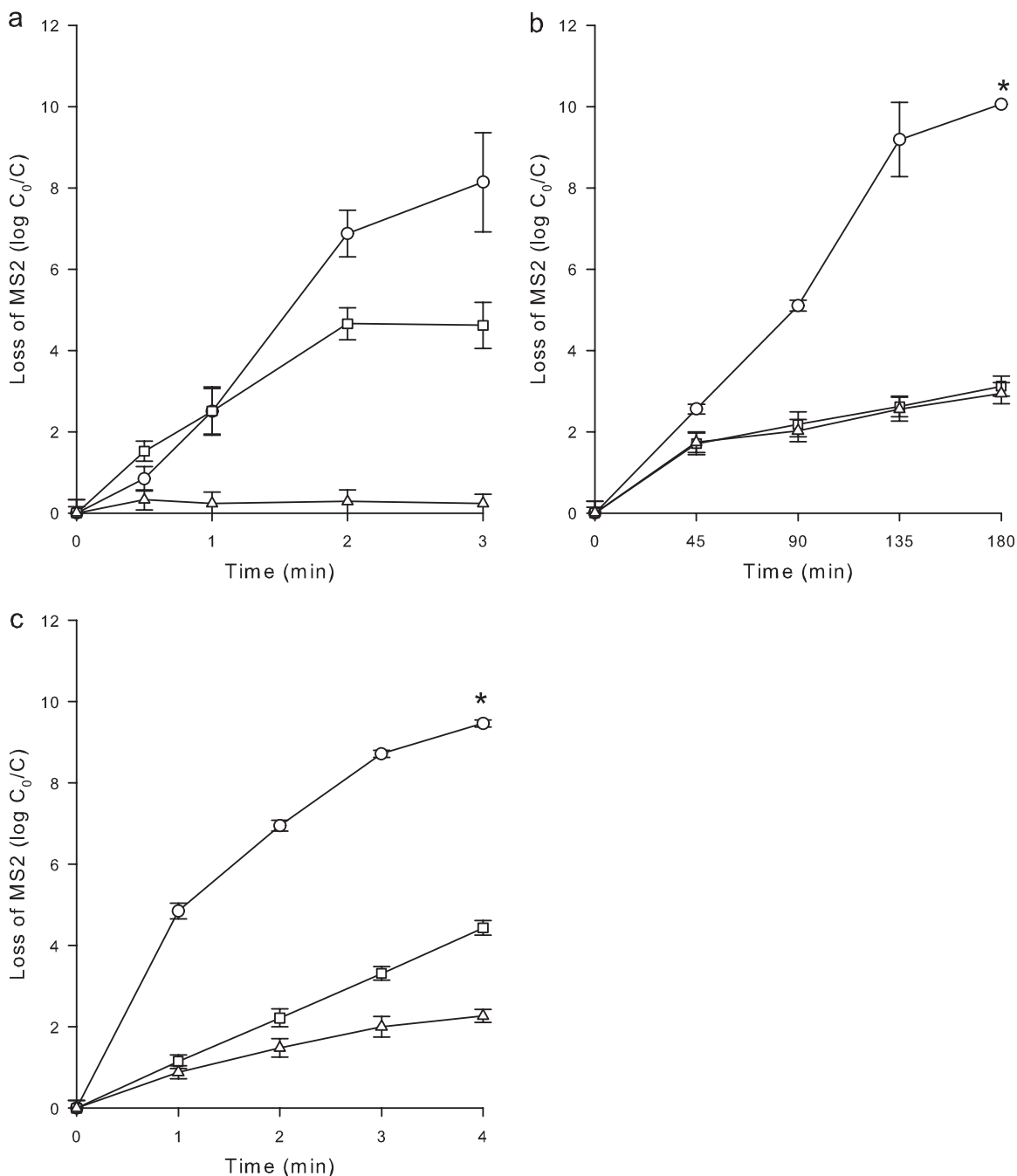


FIG. 2. Loss of infective MS2 and qPCR signal after exposure to heating at 72°C (a), singlet oxygen (b), and UV irradiation (c). The UV exposures correspond to doses of 1,900, 3,200, 4,400, and 5,900 J/m², respectively. C, culturing results; squares, ET-qPCR; triangles, qPCR without ET. Primer set 12 was used for 72°C and singlet oxygen experiments, and primer set 3 was used for UV irradiation. Error bars depict 95% confidence intervals; asterisks signify values below the detection limit.

Heat. The heat-inactivated MS2 exhibited no significant qPCR signal loss even after >8 log units of inactivation (Fig. 2a). The qPCR signals were constant and therefore independent of increases in inactivation. Thus, they could not be used to track changes in infectivity. However, coupling heat inactivation with ET caused a significant, dose-dependent increase in ET-qPCR signal loss. The loss of false-positive qPCR signal after ET was in agreement with data obtained from inactiva-

tion at 72°C of hepatitis A, poliovirus, and feline calicivirus (27).

The absence of a heat-induced effect on the qPCR results is in line with the current understanding of the mechanism of heat inactivation. Heating primarily damages viruses by denaturing the proteins that comprise the capsid (29, 34). This denaturation likely renders the capsid more susceptible to proteolytic degradation (8, 27) and may explain why the heat

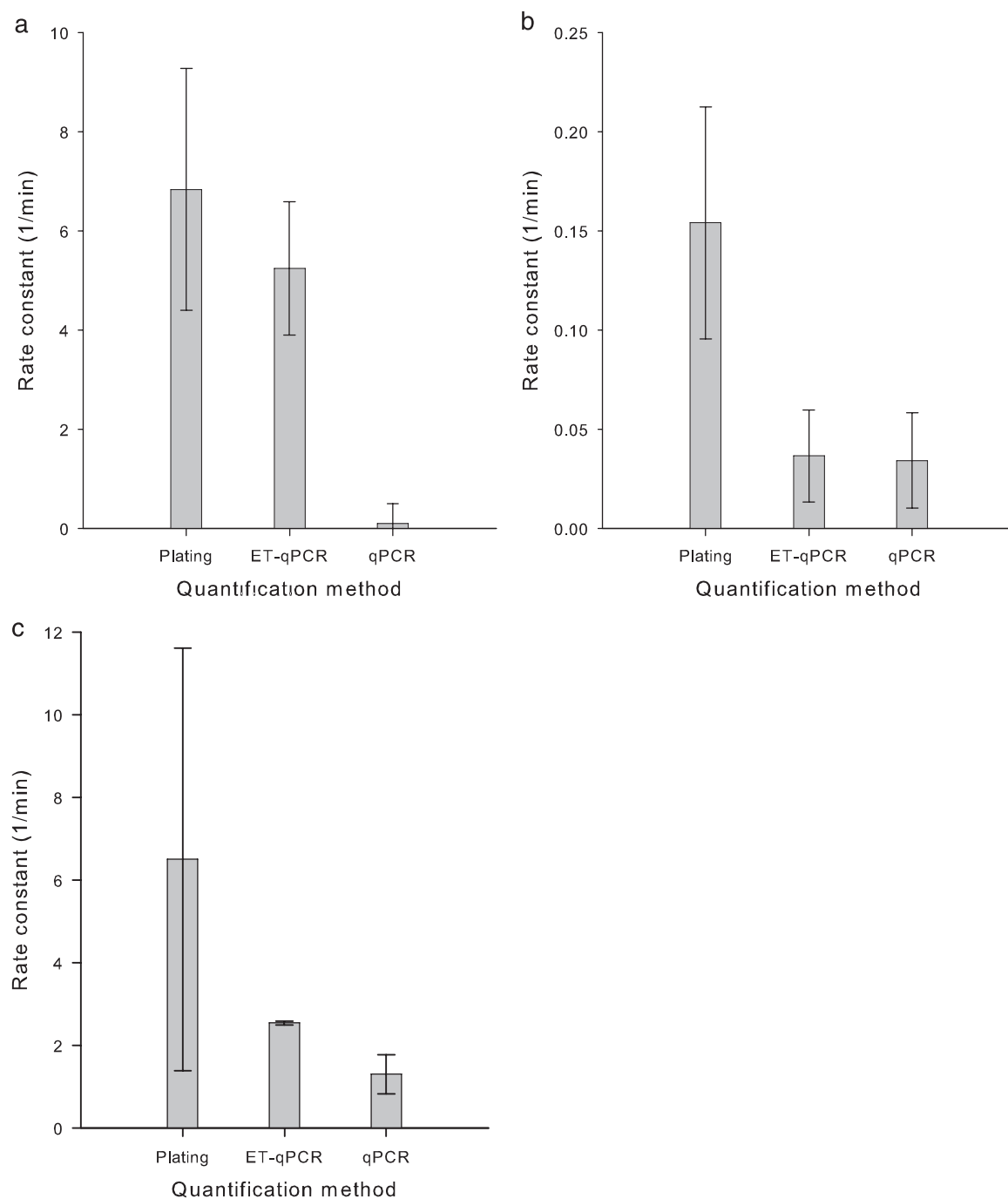


FIG. 3. First-order inactivation rate constants during treatment of MS2 with heat at 72°C (a), singlet oxygen (b), and UV irradiation (c). Error bars depict 95% confidence intervals.

treatment caused the biggest discrepancy in the qPCR results in the presence and absence of ET. Of all the inactivating treatments tested, heat likely caused the greatest denaturing of the capsid, rendering the heat-inactivated MS2 most sensitive to proteolytic and ribonucleic degradation. The net effect of this process is a large decrease in false-positive signals upon introduction of ET prior to qPCR.

We chose treatment at 72°C to produce mixed populations of infective and inactivated viruses and to avoid complete ex-

posure of the genomic RNA. A temperature of 72°C is believed to cause inactivation without complete capsid destruction (27). This assumption was supported with transmission electron micrographs of 72°C-inactivated MS2 that showed that the viruses had slightly expanded after treatment without rupturing into smaller fragments (data not shown). Treating samples for 15 to 20 s at this temperature also constitutes pasteurization, making this treatment a relevant sterilization option for a number of industries.

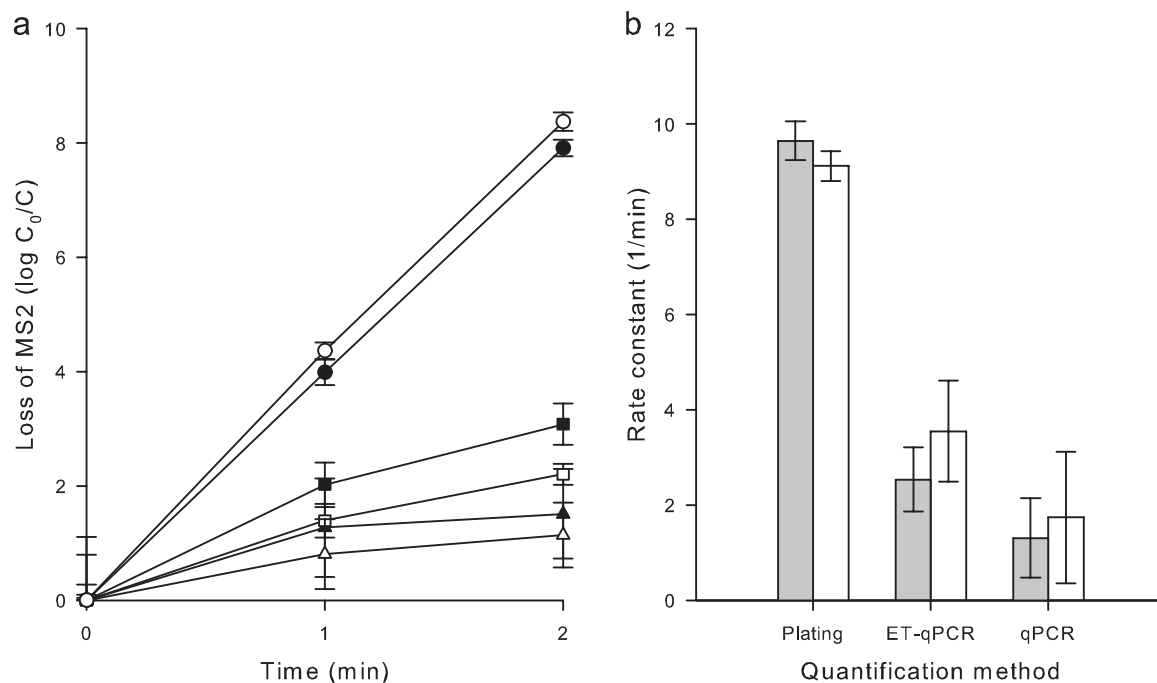


FIG. 4. Comparison of the loss of infective MS2 and qPCR signal in dilution buffer and LGW after exposure to UV irradiation and the corresponding inactivation rate constants. (a) The 1- and 2-min UV exposures corresponded to doses of 1,900 and 3,200 J/m². Circles, culturing results; squares, ET-qPCR; triangles, qPCR without ET. Open symbols are MS2 samples in dilution buffer; filled symbols are MS2 in LGW samples. (b) First-order inactivation rate constants during treatment of MS2 with UV radiation. Gray bars are MS2 samples in dilution buffer; white bars are MS2 in LGW samples. Error bars depict 95% confidence intervals.

Singlet oxygen. Singlet oxygen was chosen as a representative of ROS because it is an important species in the inactivation of viruses in sunlight-exposed surface waters (4). Furthermore, singlet oxygen and other ROS are involved in virus inactivation during advanced oxidation technologies. The singlet oxygen-inactivated samples also showed a greater loss of qPCR signal after ET (Fig. 2b). However, unlike the heat-inactivated samples, this decreased signal was seen only in a subset of the primers tested, and the magnitude of the signal loss was less than the heat-inactivated samples (Table 2). One explanation for this difference is that the high reactivity of this ROS limited its ability to diffuse through the MS2 capsid because it is instantly consumed while oxidizing the proteins. Thus, the singlet oxygen-induced effect was primarily a capsid-damaging effect. Unlike heat, however, singlet oxygen mainly modifies a small subset of amino acids (9). Therefore, the damage that it caused to the capsid was likely not intense enough to render the viruses susceptible to the ET. Instead, it may have caused damage that limited the capsid's other function, binding with its host cell. Verification of this hypothesized mechanism is currently under study.

The singlet oxygen data support the hypothesis that some treatments cause inactivation by damaging the capsid without rendering it more susceptible to proteolytic degradation. The ET-qPCR offers no advantage over PCR alone for these treatments because the ET cannot assay this type of capsid damage. It should be noted that other proteolytic enzymes may be able to make this differentiation. In the framework of this study, we tested the use of chymotrypsin, trypsin, and elastase, as well as a combination of all three, as an alternative to using proteinase

K. These enzymes were purposefully selected because they have been shown to have higher proteolytic activity than other enzymes and to be effective at degrading damaged proteins (8, 31). We found, however, that they were no more effective than proteinase K alone in reducing the false-positive qPCR signal (data not shown).

UV radiation. UV inactivation of MS2 did not result in sufficient damage to the genome to account for the loss in infectivity. For UV doses below 10,000 J/m², UV inactivation is often equated with its genome-damaging activity, e.g., the production of photoproducts such as thymine dimers or bond breakage (16, 23, 39). In the current work, however, the maximal loss of qPCR signal could account for only 4.5 of the total 8.7 log units of infectivity loss (Table 2), despite the fact that the maximal UV dose (after 4 min) was 5,900 J/m². We do not believe that this discrepancy is due to the inability of qPCR to detect UV damage (14). Therefore, the more important locus of UV damage was the capsid. This conclusion is supported by the fact that the ET caused a further decrease in qPCR signal, a situation that is dependent on capsid damage.

One possibility is that the UV produced ozone during the treatment that damaged the capsid. However, other studies have shown UV-induced capsid damage even when the formation of ozone was strictly controlled (28). This supports the hypothesis that UV damage occurred primarily by direct action on the capsid and that genome damage only partially contributes to the overall inactivation. Whether this trend holds for other types of viruses (e.g., DNA viruses) is currently under study in our lab.

Applicability of qPCR and ET-qPCR to an environmental sample. The natural organic matter (NOM) present in environmental samples is known to inhibit PCR efficiency (6). To check if lake water inhibitors altered the qPCR and ET-qPCR responses compared to controlled laboratory solutions, we conducted an inactivating treatment using a water sample from Lake Geneva as the experimental matrix. Lake Geneva serves as an important drinking water source for western Switzerland; this sample thus represents a realistic matrix in which virus concentrations may be monitored. UV radiation was chosen as the inactivating treatment because this technique is becoming increasingly popular for the disinfection of drinking water. The procedure for prefiltering and concentrating the viruses was similar to a recently reported study that also used qPCR to quantify viruses in environmental samples (42). As can be seen in Fig. 4, the inactivation rates for both the PCR and ET-qPCR in the lake water sample were not statistically different from results with the control solution. This indicates that ET-qPCR results obtained in clean laboratory experiments are directly transferable to environmental samples with a low NOM content, such as the Lake Geneva sample. The effect of environmental concentrates with a higher NOM concentration (e.g., wastewater effluent) is currently under investigation in our laboratory. If there are matrix components that affect the inactivation rates (and thus the ratio between plating and ET-qPCR), then it will be critical to determine the inactivation rates using the correct environmental matrix.

Using measurements of genetic damage to track infectivity. Our study unambiguously shows that the amount of damage to the genome greatly underestimated the level of inactivation for all the inactivating treatments studied. By using primers that span the entire coding region of the genome, we could detect damage to any one of the four genes encoded by the MS2 genome. To our knowledge, this is the first time that genomic damage has been measured across the entire coding region. In our assessment of genome damage, we made two highly conservative assumptions: first, that damage to any gene would interrupt a vital function and result in inactivation and, second, that no virus was damaged in multiple regions and, therefore, the genome-wide qPCR results could be linearly summated. Summing the qPCR signal loss after inactivating treatment (in the absence of the ET) should tell us how much genomic damage occurred from the treatment itself. It should be noted that to achieve high levels of inactivation (e.g., 10 log units), it is possible that the majority of the viruses underwent multiple inactivation "hits" to the genome before the 10¹⁰th virus was inactivated. Thus, our second assumption probably leads to an overestimation of the number of damaged genomes.

Despite the conservative nature of these assumptions, we determined that the genome damage alone could not account for the inactivation but, in fact, underestimated the total inactivation by orders of magnitude (Table 2). This is in contrast to the findings of Simonet and Gantzer (39), who suggested that genome damage could entirely account for the inactivation of UV-exposed MS2. This discrepancy may be related to differences in experimental approach: in this study 12 genome fragments of equivalent length were used, whereas Simonet and Gantzer measured six fragments of increasing length up to 1,909 bases. The differences in our findings may be related to the fact that Simonet and Gantzer extrapolated their results

to estimate the effect on the whole genome, whereas our findings are based on actual measurements of the entire coding region (representing 97% of the genome). Our findings support the hypothesis that genomic damage plays only a minor role in the total inactivation. If genomic damage cannot account for the inactivation of other viruses, then the use of qPCR and ET-qPCR to determine infectivity will be fraught with false-positive signals. An exhaustive range of alternative ET configurations should be tested to find an ET that will reliably remove the false-positive signals. However, barring the discovery of an ET-qPCR that fully eliminates this signal, our findings support the conclusion that qPCR (either alone or in conjunction with ET) may never produce results that are equivalent to infectivity assays. Our examination of the entire coding region gives the strongest evidence to date that this is the case.

A specific log loss of infectivity corresponds to an equivalent loss of ET-qPCR signal only when the ratio between the inactivation rate constants comes to unity. In this ideal situation, loss of ET-qPCR signal could be directly used to assess inactivation. However, if they are not equivalent, then approaching a 1:1 ratio increases the sensitivity of the qPCR method by allowing it to reliably detect lower levels of inactivation: if the ratio between culturing and qPCR rate constants is far removed from unity (>1), then a unit loss of infectivity corresponds to a small change in qPCR signal that is potentially difficult to quantify. This we consider to be the main advantage of the ET-qPCR method in its current form: the use of ET caused a significant decrease in the false-positive signal in 31 of the 35 samples (Fig. 2) and never contributed an additional false-positive signal. ET thus enhanced or maintained the sensitivity of the qPCR to detect infectivity after all of the inactivating treatments tested, and, therefore, should always be run prior to qPCR.

Unfortunately, the ET did not completely eliminate the false-positive qPCR signals for any of the inactivating mechanisms tested. The best correlation between the ET-qPCR and the culturing assays occurred with the heat-inactivated samples; before reaching the maximal qPCR signal loss, the two methods showed similar inactivation kinetics (Fig. 2a). After reaching this plateau, however, the ET-qPCR method failed to continue tracking infectivity. The reason for this maximum signal loss, i.e., the plateau effect, remains unresolved. As discussed above, this incomplete degradation may be related to both the secondary structure of the genome and its association with the capsid or the A protein. This may result in less RNA degradation due to the decreased access between the RNase and the genome. Nevertheless, the ratio between the culturing and ET-qPCR inactivation rate constants is often >1 . Therefore, an ET-qPCR signal loss of 4.5 log units corresponds to >4.5 log units of inactivation. Assuming treatment requirements are in the range of 5 log units of viral inactivation, ET-qPCR will have a sufficient dynamic range.

An important conclusion of this study is that, while ET-qPCR results are not identical to culturing results, ET-qPCR can be used to monitor MS2 infectivity. The ET-qPCR signal consistently decreased with inactivation after all of the treatments tested. Accordingly, the measurements of ET-qPCR could be used to track MS2 infectivity. For example, the ratio of the inactivation rate constants for culturing and ET-qPCR

after heat treatment was 1.3:1. This ratio could then be used in conjunction with the ET-qPCR results to predict the level of inactivation. For example, a decrease in the ET-qPCR signal of 2 log units would correspond to a 2.6-log loss of infectivity. The importance of the ET step is especially evident in the heat-inactivated samples. The inactivation rate constant for the qPCR alone was not different from zero, and the qPCR results could not be used to calculate inactivation. Adding ET to the qPCR method, however, gave it a powerful new capability: the ability to track the infectivity of heat-inactivated MS2.

In a less quantitative way, decreases in ET-qPCR signal could simply be used to verify changes in infectivity. For example, Baert et al. (1) also saw a dose-dependent increase in ET-qPCR signal loss upon inactivation of poliovirus with heat treatment of 80°C. Because the loss of ET-qPCR signal was not identical to the loss in infectivity, however, they concluded that there was no correlation between the qPCR and infectivity results. Contrary to the conclusions by Baert et al., we believe that the ET-qPCR signal yields valuable information regarding virus infectivity as long as it responds to inactivation in a manner proportional to the plating results, even if the proportionality factor is not unity. Indeed, this relationship was seen after all of the treatments tested, thus showing the robustness of ET-qPCR as an assay for infectivity.

Although the general trends were similar, the exact relationship between culturing and ET-qPCR differed for the three inactivating treatments tested. This is an important finding because it proves that data obtained for one form of inactivation cannot be used to assess infectivity for another form. In addition, it will likely prove incorrect to assume that the inactivation profiles can be transferred between virus species as differences in virus susceptibility have been widely reported (16, 24, 28, 40). Accordingly, if the aforementioned method is used to quantify infectivity with ET-qPCR, the relationship between the culturing and ET-qPCR inactivation curves would need to be established for each virus and inactivating treatment. This comparison would again depend on the culturability of the virus. As such, this method may not be practical for measuring multiple viruses and inactivation methods but may find an application where the inactivation of a specific virus in a given process is routinely measured. Such a situation may be encountered in the context of water treatment, where the same disinfection method is used to control a small number of regulated viruses. As a qualitative measure of inactivation, ET-qPCR yielded good results for each of the inactivating treatments considered. It could thus be used to evaluate if a given method of disinfection has any effect on virus infectivity at all or potentially even which disinfectant dose gives the most inactivation.

Additional applications of ET-qPCR. ET-qPCR may have other benefits in addition to tracking changes in virus infectivity. It may also overcome another potential limitation of the culture-based method, for example, to detect viruses that have adsorbed onto surfaces. It has been shown that viruses can reversibly adsorb onto particles without losing infectivity (35). Adsorption onto a particle may block an infective virus from physically accessing its host cell during a culture-based assay. If these viruses are released from their surfaces, they might regain the ability to infect a host cell. Thus, otherwise-infective viruses may not be detected by culturing, leading to false-

negative results. The ET-qPCR method should overcome this spatial limitation of culturing methods to detect both infective viruses adsorbed onto particles and those in solution.

ACKNOWLEDGMENTS

We thank Michel Bernard for his contributions with numerous laboratory techniques, Elena Suvorova for transmission electron microscopy work, and Barbara Morasch for her review of the manuscript.

Support for B.M.P. was provided in part by Marie Curie Fellowship grant no. 220706.

REFERENCES

- Baert, L., C. E. Wobus, E. Van Coillie, L. B. Thackray, J. Debevere, and M. Uyttendaele. 2008. Detection of murine norovirus 1 by using plaque assay, transfection assay, and real-time reverse transcription-PCR before and after heat exposure. *Appl. Environ. Microbiol.* **74**:543–546.
- Belliot, G., A. Lavaux, D. Souihel, D. Agnello, and P. Pothier. 2008. Use of murine norovirus as a surrogate to evaluate resistance of human norovirus to disinfectants. *Appl. Environ. Microbiol.* **74**:3315–3318.
- Bhattacharya, S. S., M. Kulka, K. A. Lampel, T. A. Cebula, and B. B. Goswami. 2004. Use of reverse transcription and PCR to discriminate between infectious and non-infectious hepatitis A virus. *J. Virol. Methods* **116**:181–187.
- Blough, N. V., and R. G. Zepp. 1995. Reactive oxygen species in natural waters, p. 280–333. *In* C. S. Foote, J. S. Valentine, A. Greenberg, and J. F. Liebman (ed.), *Active oxygen in chemistry*. Blackie Academic & Professional, London, United Kingdom.
- Bothner, B., and G. Siuzdak. 2004. Electrospray ionization of a whole virus: analyzing mass, structure, and viability. *ChemBioChem* **5**:258–260.
- Chandler, D. P. 1998. Redefining relativity: quantitative PCR at low template concentrations for industrial and environmental microbiology. *J. Ind. Microbiol. Biotechnol.* **21**:128–140.
- Chapron, C. D., N. A. Ballester, J. H. Fontaine, C. N. Frades, and A. B. Margolin. 2000. Detection of astroviruses, enteroviruses, and adenovirus types 40 and 41 in surface waters collected and evaluated by the information collection rule and an integrated cell culture-nested PCR procedure. *Appl. Environ. Microbiol.* **66**:2520–2525.
- Davies, K. J. A., S. W. Lin, and R. E. Pacifici. 1987. Protein damage and degradation by oxygen radicals. 4. Degradation of denatured protein. *J. Biol. Chem.* **262**:9914–9920.
- Davies, M. J. 2003. Singlet oxygen-mediated damage to proteins and its consequences. *Biochem. Biophys. Res. Commun.* **305**:761–770.
- Dreier, J., M. Stormer, and K. Kleesiek. 2005. Use of bacteriophage MS2 as an internal control in viral reverse transcription-PCR assays. *J. Clin. Microbiol.* **43**:4551–4557.
- Duizer, E., P. Bijkerk, B. Rockx, A. de Groot, F. Twisk, and M. Koopmans. 2004. Inactivation of caliciviruses. *Appl. Environ. Microbiol.* **70**:4538–4543.
- Fiers, W., R. Contreras, F. Duerinck, G. Haegeman, D. Iserentant, J. Merregaert, W. Minjou, F. Molemans, A. Raeymaekers, A. Vandenberghe, G. Volckaert, and M. Ysebaert. 1976. Complete nucleotide sequence of bacteriophage MS2 RNA: primary and secondary structure of the replicase gene. *Nature* **260**:500–507.
- Fiers, W., R. Contreras, F. Duerinck, G. Haegeman, J. Merregaert, W. Minjou, A. Raeymaekers, G. Volckaert, M. Ysebaert, J. Vandekerckhove, F. Nolf, and M. Vanmontagu. 1975. A-protein gene of bacteriophage MS2. *Nature* **256**:273–278.
- Fleige, S., V. Walf, S. Huch, C. Prgomet, J. Sehm, and M. W. Pfaffl. 2006. Comparison of relative mRNA quantification models and the impact of RNA integrity in quantitative real-time RT-PCR. *Biotechnol. Lett.* **28**:1601–1613.
- Gerba, C. P., K. R. Riley, N. Nwachuku, H. Ryu, and M. Abbaszadegan. 2003. Removal of *Encephalitozoon intestinalis*, calicivirus, and coliphages by conventional drinking water treatment. *J. Environ. Sci. Health B* **38**:1259–1268.
- Helentjaris, T., and E. Ehrenfeld. 1977. Inhibition of host-cell protein synthesis by UV-inactivated poliovirus. *J. Virol.* **21**:259–267.
- Hubaux, A., and G. Vos. 1970. Decision and detection limits for linear calibration curves. *Anal. Chem.* **42**:849–855.
- Jiang, Y. J., G. Y. Liao, W. Zhao, M. B. Sun, Y. Qian, C. X. Bian, and S. D. Jiang. 2004. Detection of infectious hepatitis A virus by integrated cell culture/strand-specific reverse transcriptase-polymerase chain reaction. *J. Appl. Microbiol.* **97**:1105–1112.
- Jursch, C. A., W. H. Gerlich, D. Glebe, S. Schaefer, O. Marie, and O. Thraenhart. 2002. Molecular approaches to validate disinfectants against human hepatitis B virus. *Med. Microbiol. Immunol.* **190**:189–197.
- Kohn, T., and K. L. Nelson. 2007. Sunlight-mediated inactivation of MS2 coliphage via exogenous singlet oxygen produced by sensitizers in natural waters. *Environ. Sci. Technol.* **41**:192–197.
- Lamhoujeb, S., I. Fliss, S. E. Ngazoa, and J. Jean. 2008. Evaluation of the persistence of infectious human noroviruses on food surfaces by using real-

- time nucleic acid sequence-based amplification. *Appl. Environ. Microbiol.* **74**:3349–3355.
22. **Lucena, F., F. Ribas, A. E. Duran, S. Skraber, C. Gantzer, C. Campos, A. Moron, E. Calderon, and J. Jofre.** 2006. Occurrence of bacterial indicators and bacteriophages infecting enteric bacteria in groundwater in different geographical areas. *J. Appl. Microbiol.* **101**:96–102.
 23. **Mamane, H., H. Shemer, and K. G. Linden.** 2007. Inactivation of *E. coli*, *B. subtilis* spores, and MS2, T4, and T7 phage using UV/H₂O₂ advanced oxidation. *J. Hazard Mater.* **146**:479–486.
 24. **Miller, R. L., and P. G. Plageman.** 1974. Effect of ultraviolet light on menogovirus: formation of uracil dimers, instability and degradation of capsid, and covalent linkage of protein to viral RNA. *J. Virol.* **13**:729–739.
 25. **Nappier, S. P., M. D. Aitken, and M. D. Sobsey.** 2006. Male-specific coliphages as indicators of thermal inactivation of pathogens in biosolids. *Appl. Environ. Microbiol.* **72**:2471–2475.
 26. **Nasser, A. M., Y. Tchorch, and B. Fattal.** 1995. Validity of serological methods (ELISA) for detecting infectious viruses in water. *Water Sci. Technol.* **31**:307–310.
 27. **Nuanualsuwan, S., and D. O. Cliver.** 2002. Pretreatment to avoid positive RT-PCR results with inactivated viruses. *J. Virol. Methods* **104**:217–225.
 28. **Nuanualsuwan, S., and D. O. Cliver.** 2003. Capsid functions of inactivated human picornaviruses and feline calicivirus. *Appl. Environ. Microbiol.* **69**:350–357.
 29. **Nuanualsuwan, S., and D. O. Cliver.** 2003. Infectivity of RNA from inactivated poliovirus. *Appl. Environ. Microbiol.* **69**:1629–1632.
 30. **Poschetto, L. F., A. Ike, T. Papp, U. Mohn, R. Bohm, and R. E. Marschang.** 2007. Comparison of the sensitivities of noroviruses and feline calicivirus to chemical disinfection under field-like conditions. *Appl. Environ. Microbiol.* **73**:5494–5500.
 31. **Prinsze, C., T. M. A. R. Dubbelman, and J. Vansteveninck.** 1990. Protein damage induced by small amounts of photodynamically generated singlet oxygen or hydroxyl radicals. *Biochim. Biophys. Acta* **1038**:152–157.
 32. **Rahn, R. O.** 1997. Potassium iodide as a chemical actinometer for 254 nm radiation: use of iodate as an electron scavenger. *Photochem. Photobiol.* **66**:450–455.
 33. **Rodriguez, R. A., I. L. Pepper, and C. P. Gerba.** 2009. Application of PCR-based methods to assess the infectivity of enteric viruses in environmental samples. *Appl. Environ. Microbiol.* **75**:297–307.
 34. **Rombaut, B., B. Verheyden, K. Andries, and A. Boeye.** 1994. Thermal inactivation of oral polio vaccine—contribution of RNA and protein inactivation. *J. Virol.* **68**:6454–6457.
 35. **Sakoda, A., Y. Sakai, K. Hayakawa, and M. Suzuki.** 1997. Adsorption of viruses in water environment onto solid surfaces. *Water Sci. Technol.* **35**:107–114.
 36. **Shiba, T., and Y. Suzuki.** 1981. Localization of A protein in the RNA-A protein complex of RNA phage MS2. *Biochim. Biophys. Acta* **654**:249–255.
 37. **Shin, G. A., and M. D. Sobsey.** 1998. Reduction of Norwalk virus, poliovirus 1 and coliphage MS2 by monochloramine disinfection of water. *Water Sci. Technol.* **38**:151–154.
 38. **Shin, G. A., and M. D. Sobsey.** 2003. Reduction of Norwalk virus, poliovirus 1, and bacteriophage MS2 by ozone disinfection of water. *Appl. Environ. Microbiol.* **69**:3975–3978.
 39. **Simonet, J., and C. Gantzer.** 2006. Inactivation of poliovirus 1 and F-specific RNA phages and degradation of their genomes by UV irradiation at 254 nanometers. *Appl. Environ. Microbiol.* **72**:7671–7677.
 40. **Smirnov, Y. A., M. P. Rodriguesmolto, and M. T. Famadas.** 1983. Protein-RNA interaction in encephalomyocarditis virus as revealed by UV light-induced covalent linkages. *J. Virol.* **45**:1048–1055.
 41. **Sobsey, M. D., D. A. Battigelli, G. A. Shin, and S. Newland.** 1998. RT-PCR amplification detects inactivated viruses in water and wastewater. *Water Sci. Technol.* **38**:91–94.
 42. **Symonds, E. M., D. W. Griffin, and M. Breitbart.** 2009. Eukaryotic viruses in wastewater samples from the United States. *Appl. Environ. Microbiol.* doi: 10.1128/AEM.01899-08.
 43. **Taverner, M. P., and E. F. Connor.** 1992. Optical enumeration technique for detection of baculoviruses in the environment. *Environ. Entomol.* **21**:307–313.
 44. **U.S. Environmental Protection Agency.** 2007. National primary drinking water regulations for lead and copper. 40 CFR part 141. U.S. Environmental Protection Agency, Washington, DC.
 45. **Williamson, K. E., M. Radosevich, and K. E. Wommack.** 2005. Abundance and diversity of viruses in six Delaware soils. *Appl. Environ. Microbiol.* **71**:3119–3125.